Analysis of Low-Order Autoregressive Models for Ultrasonic Grain Signal Characterization

Tao Wang, Jafar Saniie, *Member, IEEE*, and Xiaomei Jin

Abstract—**In testing materials nondestructively with ultrasound, the grain scattering signal provides information that may be correlated to regional microstructure variation. In the Rayleigh scattering domain, grain scattering results in an upward shift in the expected frequency of broadband echoes, while attenuation caused by scattering and absorption affects the shift in a downward direction. Both upward and downward shifts are known to be dependent on grain size distribution. In this paper, the second- and third-order autoregressive (AR) models are used to evaluate the spectral shift in grain signals by utilizing features such as resonating frequency, maximum energy frequency or AR coefficients. Then, Euclidean distance, based on these features, is applied to classify grain scattering characteristics. Using both computer simulated data and experimental results, the probability of correct classification is found to be about 75% for the second-order AR model and 88% for the third order AR model, when the conditions are such that the expected shift between the center frequency of echoes is less than 4%.**

Introduction

WHILE the ultrasonic grain scattering signal conveys microstructure information, this information is often born in such a complex manner that the signal exhibits a great deal of variability in time domain. Thus, spectral analysis is often adopted as an alternative method for signal characterization. A reasonably accurate model for the grain signal consists of a convolution of components representing the contributions of a measuring system impulse response (basic ultrasonic wavelet) and the grain scattering function [1], [2]. As shown in Fig. 1, the grain signal from a given region of the specimen can be represented as a convolution of $u(t)$, the impulse response of the measuring system, and the grain impulse response, $h(t)$, including the effects of scattering and the attenuation characteristics of the propagation path,

$$r(t) = u(t) * h(t). \tag{1}$$

The amplitude spectrum of measured data can be obtained by taking the Fourier transform of (1):

$$R(f) = U(f)\,H(f) \tag{2}$$

where [2] is

$$H(f) = \left[\langle \alpha_s(f) \rangle\, e^{-2\langle \alpha(f) \rangle x}\right]^{1/2} \sum_{k=1}^{N} \beta_k\, e^{-j2\pi f \tau_k}. \tag{3}$$

The summation in (3) represents the composite nature of backscattered echoes associated with grain scattering. The random variable N is the number of echoes detected at random arrival time, τ_k, and β_k represents the random amplitude of the detected

Manuscript received July 17, 1989; revised June 25, 1990; accepted October 29, 1990.

The authors are with the Department of Electrical and Computer Engineering, Illinois Institute of Technology, Chicago, IL 60616.

IEEE Log Number 9041513.

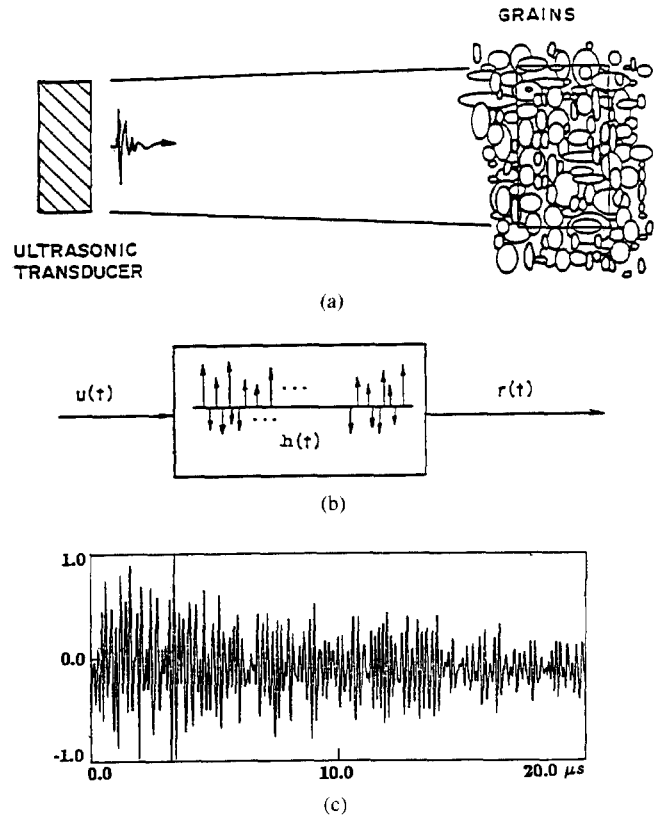

Fig. 1. (a) Range cell geometry. (b) Grain scattering model. (c) Ultrasonic measured grain signal.

echoes. The term $\langle \alpha_s(f) \rangle$ is the expected frequency-dependent scattering behavior of grains in the region of interest within the material. The term $e^{-2\langle \alpha(f) \rangle x}$ is the frequency-dependent attenuation of the echo while it propagates through the material at distance x. The shape of $U(f)$ is governed by the transfer function of the ultrasonic pulser and the transmitting/receiving transducers. Since the measuring system characteristics are fixed, the function $U(f)$ is known and is often modeled as a bandpass Gaussian shape spectrum.

Substituting (3) into (2) yields

$$R(f) = \langle U(f) \rangle \sum_{k=1}^{N} \beta_k\, e^{-j2\pi f \tau_k} \tag{4}$$

where

$$\langle U(f) \rangle = U(f) \left[e^{-2\langle \alpha(f) \rangle x} \langle \alpha_s(f) \rangle\right]^{1/2}. \tag{5}$$

In (4) and (5), the term $\langle U(f) \rangle$ is referred to as the transfer function of the expected ultrasonic wavelet in the material, including the effects of scattering and attenuation. Both the $\alpha_s(f)$

0885-3010/91/0300-0116$01.00 © 1991 IEEE

and $\alpha(f)$ are dependent on the grain size, $\bar{D}$, and the frequency of ultrasonic waves. If the measurement is in the Rayleigh scattering region [1], then,

$$\alpha(f) = c_1 f + c_2 \bar{D}^3 f^4 \tag{6}$$

where c_1 is the absorption constant, c_2 is the scattering constant, and $\langle \alpha_s(f) \rangle$ is proportional to $c_2 \bar{D}^3 f^4$.

It should be noted that the transfer function model presented here, utilizing a linear system theory, is only a heuristic model which represents the frequency dependent losses of ultrasonic energy in the propagation path. The beamwidth assumes to be much larger than the grain size where the model by no means corresponds to the individual grain size boundary or its exact position in the propagation path. However, the microstructure's backscattered echoes are a composite signal proportional to the overall characteristics of the ultrasonic measuring system in terms of bandwidth and beamwidth, the scattering properties of the propagation path, and the attenuation caused by absorption, scattering, and beam spreading (diffraction effect). Since we have confined our measurement and analysis in the far field of the transducer over a small range within the material, the beam spreading and diffraction losses are minimal. Furthermore, the parameter of interest for microstructure characterization is the frequency content of the signal which is sensitive to the dispersive properties of materials, rather than the effect of diffraction.

In the Rayleigh scattering region multiple reflections between grain boundaries are negligible and $\alpha_s(f)$ shows high sensitivity to the grain size distribution. Also, in this region, high frequency components are backscattered with larger intensity when compared with low frequency components. Consequently, this situation results in an upward shift in the expected frequency of the power spectrum of broadband echoes. Since the spectral shift is grain size dependent, the estimate of the upward shift can be used for grain size characterization. Furthermore, an inspection of (4) and (5) reveals that the term $e^{-2\langle \alpha(f) \rangle x}$ influences the frequency shift in a downward direction. The downward shift is dependent on the position of the scatterers relative to the transmitting/receiving transducer. The two opposing phenomena have important potential for evaluating grain size.

An estimation of the expected frequency shift can only be achieved from random patterns of grain scattering echoes. In this paper we examine the application of the linear predictive technique [3], a method of spectral estimation which is also known as the maximum entropy method (MEM), for grain signal characterization. In particular, linear predictive analysis is applied to grain signals using the second and third order autoregressive processes. Then, the spectral features obtained by this method are used for pattern recognition and grain size characterization. Low order AR models are used because of their computational efficiency. Furthermore, low order models emphasize a high energy frequency range and are less sensitive to random spectral peaks and pits due to the random detection of multiple interfering grain echoes. In this study, both computer-simulated data and experimental results are examined, and a Euclidean distance classifier is designed for classifying grain scattering. Methods provided in this paper are also applicable in evaluating spectral shifts resulting from ultrasonic tissue scattering used in medical imaging [7]–[10].

Linear Predictive Theory

Autoregressive techniques have been extensively applied to speech processing [4], [12], and more recently, to seismic [13] and radar signal processing [14]. The autoregressive parameter identification process is closely related to the theory of linear prediction.

Assume the measured grain signal $r(n)$ is an AR process with p parameters, then the predictive value of the sampled grain signal $\hat{r}(n)$ is defined as

$$\hat{r}(n) = -\sum_{i=1}^{p} a_i r(n-i) \tag{7}$$

where the a_i refers to the AR coefficients and the p is the order of the AR model. Then, any error between the actual value $r(n)$ and the predicted value $\hat{r}(n)$ can be given by

$$e(n) = r(n) - \hat{r}(n) \tag{8}$$

the term $e(n)$ is also known as the residual. The energy of the residual is

$$E = \sum_{n} \left[r(n) + \sum_{i=1}^{p} a_i r(n-i) \right]^2 \tag{9}$$

where Σ_n represents summation over the length of data.

The best estimate of a_i can be obtained by minimizing E, i.e.,

$$\frac{\partial E}{\partial a_i} = 0; \qquad 1 \le i \le p \tag{10}$$

which can result in [3]

$$\Phi(0, j) + \sum_{i=1}^{p} a_i \Phi(i, j) = 0; \qquad 1 \le j \le p \tag{11}$$

where the correlation function $\Phi(i, j)$ is

$$\Phi(i, j) = \sum_{n} r(n-i)\, r(n-j). \tag{12}$$

Equation (11) is known as the normal equation and can be used for solving a_i since there are p equations and p unknown AR coefficients.

If the signal is an AR process, then the optimum linear predictor parameters are the AR coefficients. These coefficients can be estimated from the sample data by using existing processing techniques such as autocorrelation, autocovariance, and the lattice method [11]–[15]. When the signal is not an AR process, but an AR model is used, the number of linear predictive parameters of the optimal predictor is generally infinite. Theoretically, as the number of the predictor parameters increases, the error will decrease. A low guess for model order results in a highly smoothed spectral estimate, and a high order introduces spurious and undesired details into the spectrum. Therefore, choosing the order of the model becomes a key problem in linear predictive analysis. For example, Fig. 2 shows a measured grain signal and several typical linear predictive spectral match processes. Fig. 2(a) is a typical example of the backscattered grain signal using a 5-MHz transducer and Fig. 2(b) is the magnitude spectrum of the grain signal in a normalized logarithmic scale. Figs. 2(c) and (d) show the spectral match for a low order AR model ($p = 2$ and 3). The low order of the AR process smoothes the randomness of the grain signal spectrum and displays the trend of spectral shift. Figs. 2(e)–(h) show the higher order (i.e., $p = 10$, 50, 100, 150) of the linear predictive spectrum match processes. As demonstrated in these figures, a higher-order of AR process introduces additional details in the spectrum due to the random detection time of interfering echoes which are not informative as far as the frequency shift is concerned and also require higher computational time. Hence, in

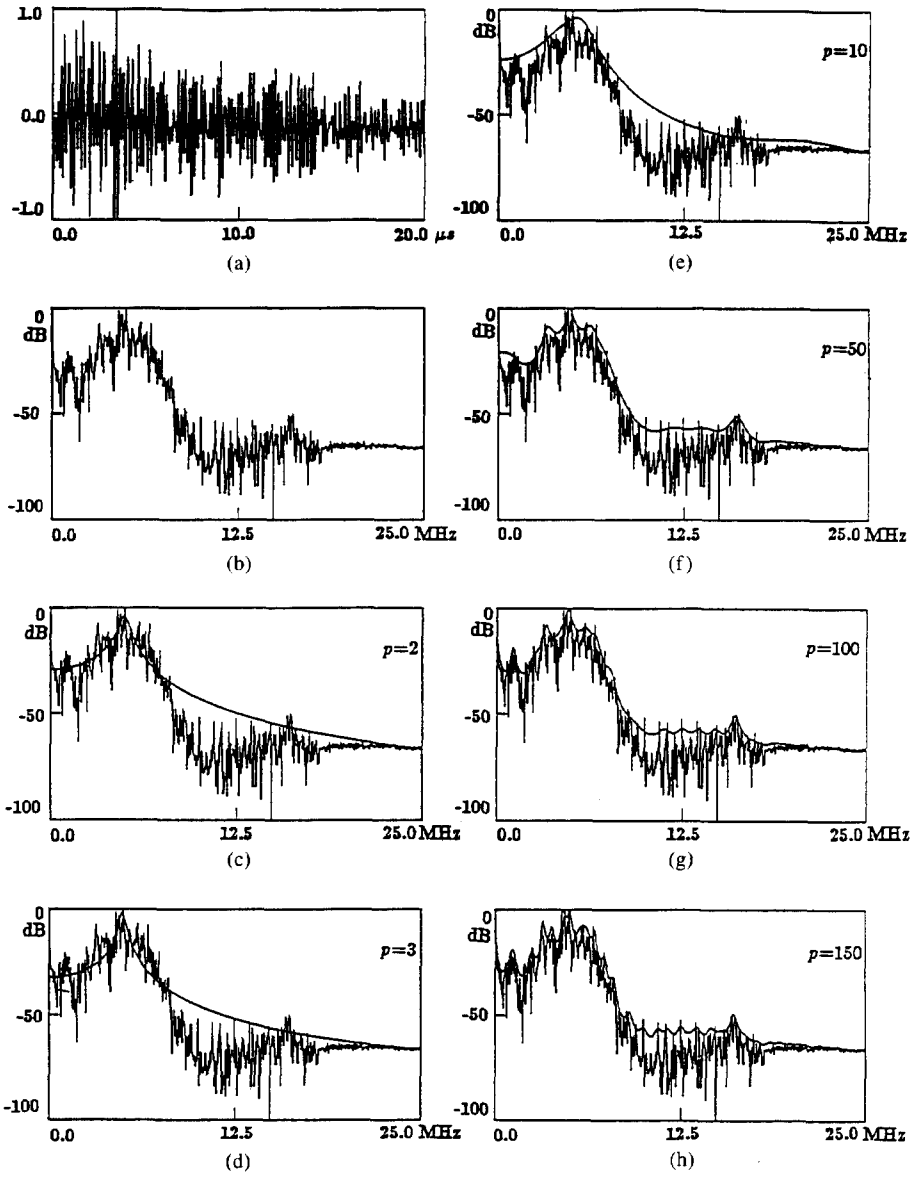

Fig. 2. (a) Backscattered ultrasonic grain signal from the steel sample. (b) Log spectrum of grain signal. (c)-(h) Log spectrum of grain signal and the AR spectral models for p = 2, 3, 10, 50, 100, and 150.

this paper, we will use both the second and third order model to characterize the spectral shift in the expected frequencies of returned echoes. A comparison between the classification performance based on the probability of error using both the second and third order model is presented.

Resonating and Maximum Energy Frequencies Relationship

It is important to point out that the linear predictive spectrum matches the signal spectrum much more closely in the frequency regions of large signal energy (i.e., near spectrum peaks). This is especially true in the case of low-order AR models. In spite of the highly smooth spectral match, second- or third-order AR models can efficiently estimate the resonating and maximum energy frequencies. Estimating resonating and maximum energy frequencies of ultrasonic echoes using second order model was studied by Kuc and Li [15]. In this section, we develop the mathematical relationships involved in the low AR models (i.e., second and third orders) to evaluate the spectral-shift for grain size classification using backscattered grain signals.

Second-Order AR Model

The general model for a discrete time grain signal $r(n)$ in a stationary segment is shown as (7). Assume the predictive error is a white noise process, then, the grain discrete transfer function, $H(z)$, for a second-order AR model can be written as [12]:

$$H(z) = \frac{1}{1 + a_1 z^{-1} + a_2 z^{-2}}. \tag{13}$$

The poles of the system are

$$z_1 = \frac{-a_1 + \sqrt{a_1^2 - 4a_2}}{2} \tag{14}$$

$$z_2 = \frac{-a_1 - \sqrt{a_1^2 - 4a_2}}{2}. \tag{15}$$

Since $H(z)$ represents the transfer function of ultrasonic echoes, which is a bandpass signal, the poles must be complex, i.e., $a_1^2 - 4a_2 < 0$. The phase of the complex poles is the resonating frequency of the second-order AR process, f_r, which can be presented as [5], [15]:

$$f_r = \frac{1}{2\pi T} \tan^{-1}\left(\frac{\sqrt{4a_2 - a_1^2}}{a_1}\right) \tag{16}$$

where T is the sampling period.

The power spectrum of the second-order model is

$$|H(f)|^2 = H(z)\, H\left(\frac{1}{z}\right)\Big|_{z = e^{j2\pi fT}}. \tag{17}$$

The maximum value of the power spectrum (i.e., maximum energy frequency) can be found by differentiating (17) with respect to f, and setting it to zero, i.e.,

$$\frac{\partial}{\partial f}\left[\frac{1}{1 + a_1 e^{-j2\pi fT} + a_2 e^{-j4\pi fT}} \cdot \frac{1}{1 + a_1 e^{j2\pi fT} + a_2 e^{j4\pi fT}}\right] = 0. \tag{18}$$

The solution to (18) results in,

$$f_m = \frac{1}{2\pi T} \cos^{-1}\left(\frac{a_1 a_2 + a_1}{-4a_2}\right). \tag{19}$$

In general, the maximum frequency, f_m, is not equal to the resonating frequency, f_r [5], [6], [15]. As shown in Fig. 3, the phase of poles is the resonating frequency. The maximum energy frequency is defined as the phase in which the product of distance from the point at unit circle to the poles is minimum. When the bandwidth of the system decreases (this situation occurs as poles approach to the unit circle, i.e., $a_2 \to 1$), the f_m will approach to f_r. This can be confirmed by evaluating (16) and (19).

The difference between the maximum energy at the frequency f_m and the resonating frequency f_r is

$$|f_r - f_m| = \frac{1}{2\pi fT}\left|\cos^{-1}\left[\frac{-1}{8a_2\sqrt{a_2}}\left[a_1^2(1 + a_2) + \sqrt{(4a_2 - a_1^2)\left(16a_2^2 - a_1^2(1 + a_2)^2\right)}\right]\right]\right|. \tag{20}$$

The numerical evaluation of (20) is shown in Fig. 4. This figure indicates that the normalized difference between f_r and f_m is small for a range of typical values of a_1 and a_2 (A typical range for a_1 is $-1.9 < a_1 < -1.6$, and for a_2 is $0.9 < a_2 < 0.99$). This implies that the resonating frequency of a second-order AR system can be approximately represented by the frequency of the maximum energy, and can also be correlated to the frequency shift inherent to random grain signals.

Third-Order AR Model

A closer spectral match can be obtained using a third-order autoregressive system:

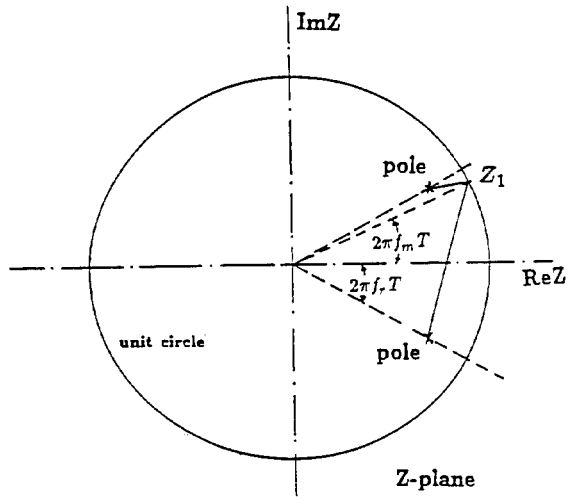

Fig. 3. Relation between the resonating frequency and the maximum-energy frequency for the second-order AR model.

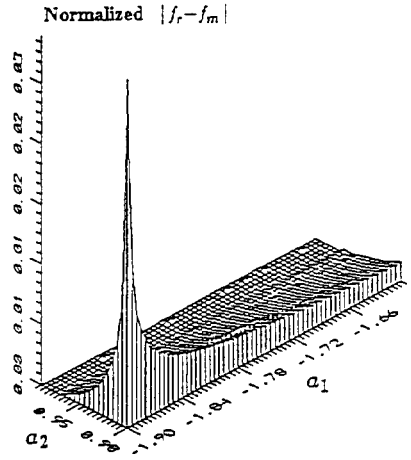

Fig. 4. Normalized difference between the resonating frequency and the maximum-energy frequency for a second-order AR model.

$$H(z) = \frac{1}{1 + a_1 z^{-1} + a_2 z^{-2} + a_3 z^{-3}}. \tag{21}$$

According to Cardino's formulas [17], the general expressions for the poles of (21) are

$$z_1 = \left[-\frac{q}{2} + \sqrt{\Delta}\right]^{1/3} + \left[-\frac{q}{2} - \sqrt{\Delta}\right]^{1/3} - \frac{a_1}{3} \tag{22}$$

$$z_2 = \frac{-1 + i\sqrt{3}}{2}\left[-\frac{q}{2} + \sqrt{\Delta}\right]^{1/3} + \frac{-1 - i\sqrt{3}}{2} \cdot \left[-\frac{q}{2} - \sqrt{\Delta}\right]^{1/3} - \frac{a_1}{3} \tag{23}$$

$$z_3 = \frac{-1 - i\sqrt{3}}{2}\left[-\frac{q}{2} + \sqrt{\Delta}\right]^{1/3} + \frac{-1 + i\sqrt{3}}{2} \cdot \left[-\frac{q}{2} - \sqrt{\Delta}\right]^{1/3} - \frac{a_1}{3} \tag{24}$$

where

$$p = a_2 - \frac{a_1^2}{3} \tag{25}$$

$$q = a_3 - \frac{a_1 a_2}{3} + \frac{2a_1^3}{27} \tag{26}$$

and

$$\Delta = \left(\frac{q}{2}\right)^2 + \left(\frac{p}{3}\right)^3 \tag{27}$$

If $\Delta < 0$, (21) will have three real poles, and the system has no resonating frequency. Note that ultrasonic echoes are bandpass signals that have resonating frequencies. Therefore, $\Delta > 0$ and under this condition, the pole z_1 will be real while z_2 and z_3 will be a pair of complex conjugate poles. The resonating frequency specified by the complex conjugate poles will be

$$f_r = \frac{1}{2\pi T} \tan^{-1}\left[\frac{3\sqrt{3}\,(A - B)}{2a_1 - 3(A + B)}\right] \tag{28}$$

where

$$A = \left|-\frac{q}{2} + \sqrt{\Delta}\right|^{1/3} \tag{29}$$

$$B = \left|\frac{q}{2} + \sqrt{\Delta}\right|^{1/3}. \tag{30}$$

The maximum energy frequency of a third-order system can be obtained by taking a derivative of the power spectrum with respect to f, and setting it equal to zero, that is,

$$\frac{\partial}{\partial f}\left|H(e^{j2\pi fT})\,H(e^{-j2\pi fT})\right| = 0. \tag{31}$$

After a number of algebraic steps, solutions for the maximum energy frequency can be obtained:

$$f_m = \frac{1}{2\pi fT} \cos^{-1}\left\{\frac{1}{2a_3}\left[-\frac{1}{3}(a_1a_3 + a_2) + \sqrt{\frac{1}{9}(a_1a_3 + a_2)^2 - \frac{1}{3}(a_1a_2a_3 + a_2a_3^2 + a_1a_3 - 3a_3^2}\right]\right\}. \tag{32}$$

Similar to a second-order AR model, the third-order model results in different maximum energy and resonating frequencies. Through an analysis of a large number of computer simulated data, the normalized difference of these two parameters ($|f_r - f_m|$) were found to be less than 20%, and the estimated values for both f_r and f_m were also found to be highly correlated with the actual center frequency of ultrasonic wavelets. The plots of normalized $|f_r - f_m|$ as a function of a_1 and a_2 for two different values of a_3 are shown in Figs. 5(a) and (b). These figures indicate that, using the third-order AR model, the difference of f_r and f_m can vary in a range of 3 to 15% or possibly higher. Furthermore, this difference is much larger than that which exists between f_r and f_m when a second-order model is used (see Fig. 4).

Computer Simulation

In our earlier study [19], it was shown that grain scattering influences the frequency content of detected echoes. Backscattered echoes from specimens with different grain sizes result in different values for the resonating frequency, the maximum energy frequency, and AR coefficients. Therefore these parameters are examined in order to find their correlations to the grain size distribution. In order to classify the specimens with different grain sizes, a Euclidean distance classifier, D_j, which measures the distance between the class j with the clustering center, $\bar{a}_{ij}$ and the estimated parameters a_i [18], is used,

$$D_j = \left[\sum_{i=1}^{p} (a_i - \bar{a}_{ij})^2\right]^{1/2} \tag{33}$$

where p is the number of parameters, and, if the AR coefficients are used, p also represents the order of the AR model. In this study, the clustering center, $\bar{a}_{ij}$, is computed using a set of training signals.

Computer simulations were used in evaluating the performance of the second- and third-order linear predictive models for classifying the grain signals representing different grain sizes. The simulation was implemented based on the principle that different grain sizes backscatter echoes with different shifts in their expected frequencies. Thus, by generating grain signals with different center frequencies, backscattered signals from specimens with different grain sizes can be simulated. The grain signals were generated by superimposing multiple echoes with random positions and amplitudes. It is assumed that the transfer function of the expected ultrasonic wavelets, $\langle U(f)\rangle$, are Gaussian in shape with center frequencies of 5.0, 5.2, and 5.4, MHz, and 3dB bandwidth of 2.5 MHz. The entire simulated data is made up of 2048 sample points with a 100 MHz sampling rate. It is also assumed that about 512 random echoes will be detected by the transducer in the duration of 20.48 μs of the backscattered signal. To depict the amplitude intensity of the detected echoes, a random number generated with a Rayleigh probability distribution is used [2]. In addition, a uniformly distributed random number generator is used for determining the position of the scatterers. The Euclidean distance classifier utilized in this study measures the distance between two sets of linear predictive parameters or the differences between the resonating frequencies, or between the frequencies of maximum energy. The decision is made based on the nearest neighbor rule. The cluster centers are formed by using fifteen sets of training data (i.e., five sets for each cluster center).

Tables I-A and I-B present the estimated mean values of the resonating and maximum energy frequencies for second- and third-order AR models along with their standard deviations. As shown in this table, both estimated resonating and maximum energy frequencies are closely related to the actual value of simulated center frequencies, although consistently biased. Furthermore, estimates are consistent since the variances are very small and can be considered to be negligible in comparison with the actual value of estimates. For example, the estimated resonating frequencies and maximum energy frequencies of a second-order AR method are consistently higher than the actual center frequencies with nearly the same variances. However, estimated resonating frequencies and maximum energy frequencies of a third-order AR model have a different tendency. The estimated resonating frequencies show a low bias with the actual center frequencies, while the maximum energy frequencies show a higher bias for all three classes of signals with very

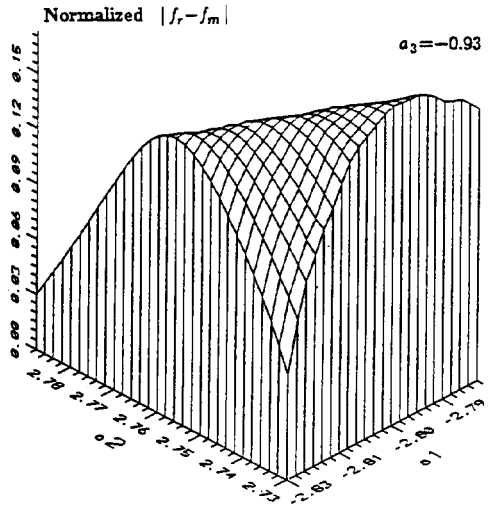

(a)

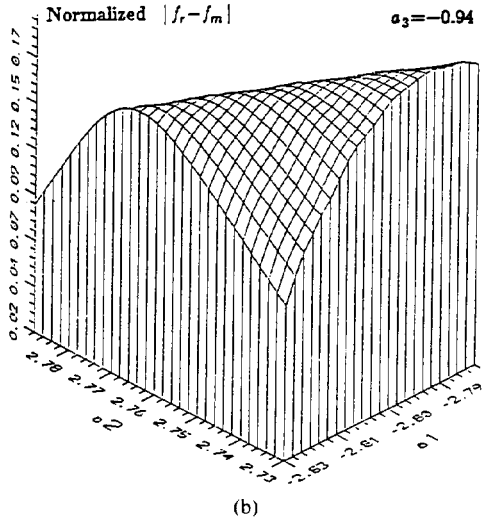

(b)

Fig. 5. Normalized difference between the resonating frequency and the maximum-energy frequency for a third-order AR model. (a) When $a_3 = -0.93$. (b) When $a_3 = -0.94$.

TABLE I
THE ESTIMATED RESONATING AND MAXIMUM-ENERGY FREQUENCIES

A—Second-Order Model

Center Frequency	Resonating Frequency	Maximum-Energy Frequency
5.0 MHz	5.12 MHz ± 0.0053	5.14 MHz ± 0.0053
5.2 MHz	5.31 MHz ± 0.0058	5.35 MHz ± 0.0058
5.4 MHz	5.52 MHz ± 0.0062	5.55 MHz ± 0.0062

B—Third-Order Model

5.0 MHz	4.67 MHz ± 0.0041	5.60 MHz ± 0.0074
5.2 MHz	4.82 MHz ± 0.0042	5.82 MHz ± 0.0065
5.4 MHz	4.97 MHz ± 0.0042	6.04 MHz ± 0.0065

small variances. It is evident from Tables I-A and I-B that the estimate of resonating frequencies or maximum energy frequencies tracks or correlates with the actual simulated center frequencies. Consequently, these estimates can be used as features representing the spectral properties of the random grain signal.

TABLE II
CLASSIFICATION RESULTS[a]

A—Using AR Coefficients

74.5% (second-order model)
88.3% (third-order model)

B—Using Resonating Frequencies

76.5% (second-order model)
81.7% (third-order model)

C—Using Maximum-Energy Frequencies

78.3% (second-order model)
81.7% (third-order model)

[a]Where the parameters are the probability of correct decision.

Furthermore, the estimation of both resonating and maximum energy frequencies for a second-order AR model follows the actual center frequency much more closely and consistently than that of a third-order AR model. This observation implies that in order to estimate the center or maximum energy frequencies, the second order model would be a better choice, and is consistent with the work of Kuc and Li [15] who used a second-order AR model for estimating center frequency.

Table II shows the classification results using second- and third-order AR models for three classes of signals with center frequencies 5, 5.2, and 5.4 MHz. Tables II-A–II-C present the classification results using AR coefficients, resonating frequencies and maximum energy frequencies, respectively. The results shown in the tables confirm that low order linear predictive models (AR) can effectively characterize the random grain signals. A comparison of the results for second- and third-order AR models indicates that the probability of correct classification of the third-order AR model is higher than that of the second-order AR model. That is expected since the third-order AR model extracts more frequency information from the random spectrum than the 2nd order AR model.

The computer simulation shows that misclassification is most likely to occur in the region between two adjacent frequency classes, (e.g., 5.0 and 5.2 MHz or 5.2 and 5.4 MHz). This observation indicates that, when the frequency difference between the two adjacent signal classes increases, the misclassification will decrease. Hence the probability of error will approach zero as the frequency difference among the classified signals increases to a certain value. For example, only four out of 30 sets of data were misclassified and all misclassification results are between adjacent classes: 5.0 and 5.2, or 5.2 and 5.4 MHz. Similar observations can be made by examining the scatter plots for AR coefficients. In particular, the scatter plot for the third order model is shown in Fig. 6 and confirms earlier discussions. A further inspection of Fig. 6 reveals that a_1 and a_2 individually show a good sensitivity to the frequency content of the signal, while the parameter a_3 is rather insensitive. Nevertheless, the feature including a_1, a_2, and a_3 will provide the best classification outcome at a relatively insignificant additional computational time. It should be noted that the simulated backscattered signal contains only multiple echoes reflected from multiple scatterers and no additional noise due to the measuring system has been considered. Therefore, in the

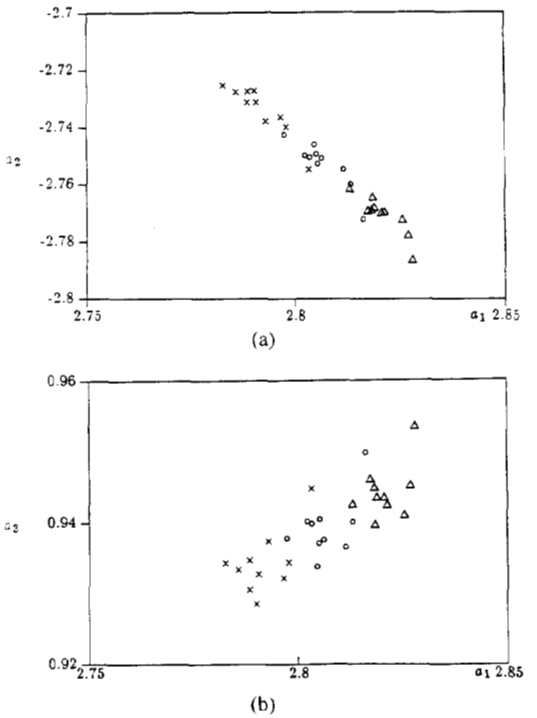

Fig. 6. Third-order AR scatter plots using the computer simulated data. (Δ for 5.0 MHz class, $\bigcirc$ for 5.2 MHz class and $\times$ for 5.4 MHz class.) (a) Scatter plot of features (a_1, a_2). (b) Scatter plot of features (a_1, a_3).

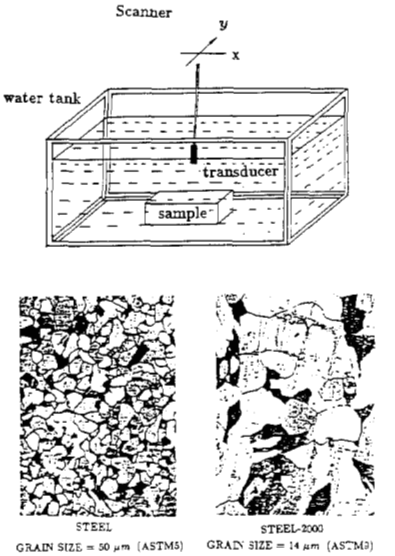

Fig. 7. Experimental setting and the micrographs of steel blocks.

presence of measuring noise, estimation errors of AR parameters become significant and as a result the performance of classification will deteriorate.

Results shown in Table II suggest that the classification performance with AR coefficients, resonating and maximum energy frequencies are nearly the same for the second-order AR model, with the slight difference being caused by an estimation error or by the relatively small number of training patterns used for this study. The probabilities of correct classification by using the AR coefficients, the resonating frequency and the maximum energy frequency are significantly different for third-order AR model. This is not surprising since both the resonating and maximum energy frequencies are functions of AR coefficients (see (28) and (32)) and represent only a reduced feature vector of the estimated AR coefficients. As a result, classification performance will degrade, although this degradation is not that significant. Another interesting observation worth noting is that the second-order AR model more closely follows the center frequency than the third-order AR model. This could be because the third-order AR model matches the random pattern more closely than the second-order model. As a result, the contribution of random pattern to the estimated AR coefficients can cause an error in the estimate of center or maximum energy frequencies. In summary, the classification results shown in Table II reveal that the feature vector formed by AR coefficients can effectively characterize the frequency difference of the grain signals, and the correct classification can be as much as 88% for the situation in which the frequency shift is less than 4%.

Experimental Results

The experimental studies were conducted using a Panametric broadband transducer with 6.22-MHz center frequency and a 3-dB bandwidth of 2.75 MHz. Two specimens examined in this study are steel blocks type 1018. One steel block has an average grain size of 14 μm (referred to as "Steel") and the other was heat-treated at 2000°F, resulting in an average grain size of 50 μm (referred to as "Steel-2000"). The grain size of the samples was analyzed by the intercept method that corresponds to the average grain boundary spacing [20]. The micrographs and general equipment setting are shown in Fig. 7. The specimens were placed at the far field of the transducer and data was acquired with a 100-MHz sampling frequency. The experiments with the same equipment setting (i.e., the same sampling rate, trigger level, damping and gain) were repeated at 20 different locations for each specimen. These 20 observations are used to design and test the performance of the classifier using AR coefficients. The measured data were obtained at different locations to ensure that the correlation among the backscattered data would be minimal. This is important for our evaluation since a class of diversified signals is capable of providing more unbiased results. Each measurement was obtained by averaging 256 measurements in order to eliminate system noise, and each data string consists of 2048 samples.

The experimental results were processed in order to obtain the linear predictive coefficients, resonating frequency and maximum energy frequency. Fig. 8 shows the scatter plot of the third AR coefficients using experimental data. This figure reveals that any two parameters (a_1 or a_2) or (a_1 or a_3) are insufficient to display the scattering characteristics of specimens with different grain sizes. To form the cluster center of different grain signals, five sets of the measurements have been used as training patterns while the remaining fifteen sets of grain signals were used for classification. Probabilities of correct classification were computed using the simple Euclidean distance as described in (33) and the final results were tabulated in Tables III and IV. An inspection of results given in Table III reveals that the difference between the estimation of resonating frequency and the maximum energy frequency for a second-order AR model is smaller than that of a third-order AR model. This is not surprising since the real pole in a third-order model contributes to the estimation of maximum energy frequency (for clarification, see (32)). Another important observation one can make from the values given in Table III is that both the resonating frequency and maximum energy frequency are shifted down as

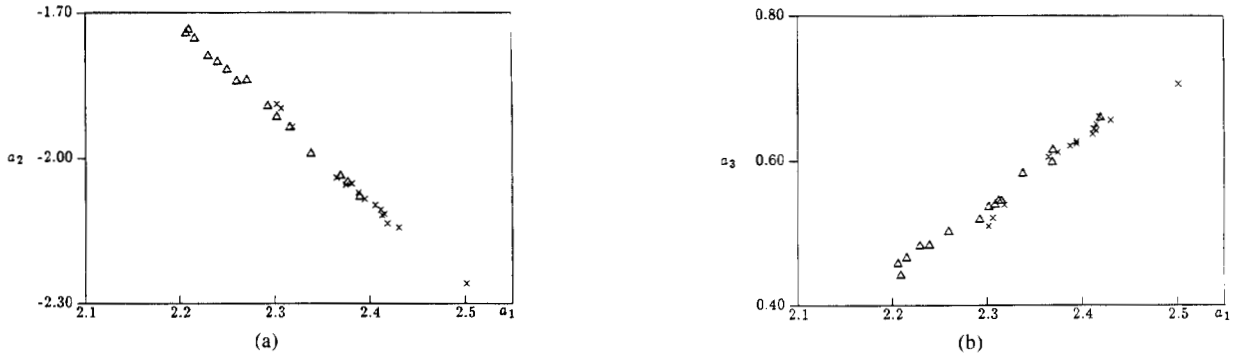

Fig. 8. Third-order AR scatter plots using experimental data. (Δ for the steel block, and $\times$ for the steel-2000 block.) (a) Scatter plot of features (a_1, a_2). (b) Scatter plot of features (a_1, a_3).

TABLE III
THE ESTIMATED RESONATING AND MAXIMUM-ENERGY FREQUENCIES (EXPERIMENTAL DATA)

Samples (Steel)	Estimated Resonating Frequency	Estimated Maximum-Energy Frequency
Steel	6.32 MHz ± 0.0215	6.31 MHz ± 0.0220 (second order-model
	6.13 MHz ± 0.0072	6.97 MHz ± 0.0197 (third-order model)
Steel-2000	5.68 MHz ± 0.0362	5.63 MHz ± 0.0388 (second-order model)
	6.03 MHz ± 0.0177	6.87 MHz ± 0.0494 (third-order model)

TABLE IV
CLASSIFICATION RESULTS USING EXPERIMENTAL DATA

Parameters	AR Coefficient	Resonating Frequency	Maximum-Energy Frequency
Probability of Correct Decision	72.5%	67.5%	67.5% (second-order model)
Probability of Correct Decision	85.0%	62.5%	67.5% (third-order model)

the grain size increased from 14 μm (Steel) to 50 μm (Steel-2000). This observation is consistent with our previous investigation performing spectral analysis using homomorphic processing [5], [19]. An inspection of standard deviation suggests that the estimates of resonating frequency and maximum energy frequency are highly consistent in spite of random patterns of grain scattering. This can be confirmed by evaluating the ratio of standard deviation of estimation over the expected value. Using the values given in Table III, this ratio is less than 1%.

Consistent estimates of AR coefficients, resonating frequencies and maximum energy frequencies, make them suitable for grain scattering feature vectors to be used for classification. The results given in Table IV indicate that resonating and maximum energy frequencies for both second- and third-order AR systems can classify the grain scattering signals effectively with a probability of correct classification higher than 62%. Better classification performance can be obtained using AR coefficients. The probability of correct classification with a third-order model is 85%, significantly higher than that of the second-order model at 72.5%. This implies that, by increasing the order of the AR model, the frequency information extracted from the random signal is increased that can result in obtaining a better classification.

CONCLUSION

In this paper, we have developed a mathematical basis for second and third order autoregressive models to evaluate the spectral shift in grain signals. Grain signal characterization is performed utilizing a Euclidean distance classifier based on AR coefficients, resonating and maximum energy frequencies. Comparisons of performances between two AR models have also been provided. Results obtained from both computer simulated and experimental data are very encouraging, and the probability of correct classification is found to be as high as 88% for the third-order model under the condition in which the

expected frequency shift is less than 4%. Further improvement can be expected by increasing the order of the AR processes, which demands a higher computational effort. This analysis has application for investigations characterizing the microstructure of materials and for ultrasonic tissue characterization.

REFERENCES

[1] J. Saniie and N. M. Bigutay, "Quantitative grain size evaluation using ultrasonic backscattered echoes," *J. Acoust. Soc. Amer.*, vol. 80, pp. 1816–1824, Dec. 1986.

[2] J. Saniie, T. Wang, and N. M. Bilgutay, "Statistical evaluation of backscattered ultrasonic grain signals," *J. Acoust. Soc. Amer.*, vol. 84, pp. 400–407, July 1988.

[3] J. Makhoul, "Linear prediction: A tutorial review," *IEEE Proc.*, vol. 63, pp. 561–580, 1975.

[4] J. D. Markel and A. H. Gray, Jr., *Linear Prediction of Speech*. Berlin: Springer-Verlag, 1982.

[5] J. Saniie, T. Wang, X. Jin, and N. M. Bilgutay, "Application of linear predictive analysis in ultrasonics grain signal characterization," *Review of Progress in Quantitative Nondestructive Evaluation*, vol. 8, D. O. Thompson and D. E. Chimenti, Eds. New York: Plenum, 1989.

[6] T. Wang, "Ultrasonic signal processing and pattern recognition in evaluating the microstructure of materials," Ph.D. dissertation, Illinois Institute of Technology, Chicago, 1987.

[7] M. Fink, F. Hottier and J. F. Cardoso, "Ultrasonic signal processing for *in vivo* attenuation measurement," *Ultrason. Imaging*, vol. 5, pp. 117–135, 1983.

[8] P. A. Narayana and J. Ophir, "Spectral shifts of ultrasonic propagation: A study of theoretical and experimental methods," *Ultrason. Imaging*, vol. 5, pp. 22–29, 1983.

[9] F. Lizzi, L. Katz, L. St. Louis, and D. J. Coleman, "Application of spectral analysis in medical ultrasonography," *Ultrason.*, pp. 77–80, Mar. 1987.

[10] R. Kuc, "Processing of diagnostic ultrasound signals," *IEEE Acoust., Speech, Signal Processing Mag.*, pp. 19–26, Jan. 1984.

[11] S. M. Kay and S. L. Marple, Jr., "Spectrum analysis—A modern perspective," *IEEE Proc.*, vol. 69, pp. 1380–1419, Nov. 1981.

[12] L. R. Rabiner and R. W. Schafter, *Digital Processing of Speech Signals*. Englewood Cliffs, NJ: Prentice-Hall Inc., 1978.

[13] T. H. Wu and A. Eljandali, "Use of time series in geotechnical data analysis," *Geotechnical Testing J.*, GTJODJ, vol. 8, pp. 151–158, Dec. 1985.

[14] Simon Haykin, "Radar signal processing," *IEEE Acoust., Speech, Signal Processing Mag.*, pp. 2–18, Apr. 1985.

[15] R. Kuc and H. Li, "Reduced-order autoregressive modeling for center frequency estimation," *Ultrason. Imaging*, pp. 244–251, July 1985.

[16] D. E. Littlewood, *A University Algebra*. London: William Heinmann, LTD., 1950.

[17] I. N. Bronshtein and K. A. Semendyayev, *Handbook of Mathematics*. New York: Van Nostrand Reinhold, 1985, pp. 119–123.

[18] K. Fukunaga, *Introduction to Statistical Pattern Recognition*. New York: Academic, 1972.

[19] J. Saniie, T. Wang, and N. M. Bilgutay, "Analysis of homomorphic processing for ultrasonic grain signal characterization," *IEEE Trans. Ultrason. Ferroelec. Freq. Contr.*, vol. 36, pp. 365–375, May 1989.

[20] J. E. Hilliand, "Grain size estimation by the intercept method," Northwestern University, Dept. Materials Science and Materials Research Center (Int. Rep.), Evanston, IL, Nov. 1963.

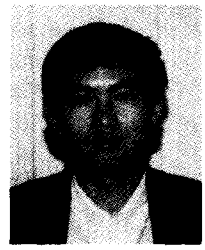

Tao Wang was born in Sijiazhuang, Hebei, China on November 4, 1965. He received the B.S. degree in electrical engineering from the University of Science and Technology of China, Hefei, Anhui, China, in 1982, and the M.S. and Ph.D. degrees, both in electrical engineering, from the Illinois Institute of Technology, in 1984 and 1987, respectively.

From 1988 to 1989, he was a postdoctoral research fellow with the Department of Electrical and Computer Engineering at Illinois Institute of Technology. Since October 1989, he has been an Ultrasonic Systems Scientist with Physical Acoustics Corporation. His research interests are digital signal processing, ultrasonic imaging, statistical pattern recognition and communication systems.

Jafar Saniie (S'80–M'81) was born in Iran on March 21, 1952. He received the B.S. degree in electrical engineering from the Univeraity of Maryland, College Park, 1974. In 1977 he received the M.S. degree in biomedical engineering from Case Western Reserve University, Cleveland, OH, and, in 1981, the Ph.D. degree in electrical engineering from Purdue University, West Lafayette, IN.

In 1981 he joined the Applied Physics Laboratory, University of Helsinki, Finland, to conduct research in photothermal and photoacoustic imaging. Since 1983 he has been with the Department of Electrical and Computer Engineering, Illinois Institute of Technology, Chicago, where he is Associate Professor and Director of the Ultrasonic Information Processing Laboratory. His current research activities include radar signal processing, estimation and detection, ultrasonic imaging, computer tomography, nondestructive testing, and digital hardware design.

Dr. Saniie is a member of the American Society for Engineering, Sigma Xi, Tau Beta Pi, Eta Kappa Nu, and has been IEEE Student Branch Counselor since 1983. He is the 1986 recipient of the Outstanding IEEE Student Counselor Award.

Xiaomei Jin was born in Hunan, China. She received the B.S. degree in electrical engineering from the University of Electronic Science and Technology of China, Chengdu, China, in 1983, and an M.S. degree in electrical engineering from Illinois Institute of Technology, Chicago, IL, in 1986. She is currently working toward the Ph.D. degree in electrical engineering at Illinois Institute of Technology, Chicago.

Her current interests include digital signal processing, ultrasonic imaging, statistical pattern recognition and communication systems.